High Temp. Mater. Proc., Vol. **30** (2011), pp. 139–144 DOI 10.1515/HTMP.2011.020

Thermal and Optical Properties of New Poly(amide-imide)/Nanocomposite Reinforced by Layer Silicate Containing Diphenyl Ether Moieties

Khalil Faghihi,[1,*] **Ellahe Faramarzi**[1] **and Meisam Shabanian**[2]

[1] Polymer Research Laboratory, Department of Chemistry, Faculty of Science, Islamic Azad University, Arak Branch, Arak, Iran

[2] Department of Chemistry, Farahan Branch, Islamic Azad University, Farmahin, Iran

Abstract. New poly(amide-imide)-montmorillonite reinforced nanocomposites containing Bis(4-N-trimellitylimido)diphenyl ether moiety in the main chain were synthesized by a convenient solution intercalation technique. Poly(amide-imide) (PAI) 4 was synthesized by the direct polycondensation reaction of Bis(4-N-trimellitylimido)diphenyl ether 3 with 4,4'-diamino diphenyl ether 2 in the presence of triphenyl phosphite (TPP), $CaCl_2$, pyridine and N-methyl-2-pyrrolidone (NMP). Morphology and structure of the resulting PAI-nanocomposite films 4a and 4b with 10 and 20 mass % silicate particles respectively, were characterized by FT-IR spectroscopy, X-ray diffraction (XRD) and scanning electron microscopy (SEM). The properties of nanocomposites films were investigated by using Uv-vis spectroscopy, thermogravimetric analysis (TGA) and water uptake measurements.

Keywords. Poly(amide-imide), montmorillonite, nanocomposite, optical and thermal properties.

1 Introduction

The properties of polymers are enhanced by the incorporation of inorganic additives. The main challenge in this area is to obtain significant improvements in the interfacial adhesion between the polymer matrix and filler since both the phases are incompatible. Polymer composites with interphase bonding have better properties, such as high modulus, strength, stiffness, and barrier and heat resistance, compared to traditional polymer macrocomposites [1–11].

Unique properties of the nanocomposites are usually observed when the ultra fine silicate layers are homogenously dispersed throughout the polymer matrix at nanoscale. The uniform dispersion of silicate layers is usually desirable for maximum reinforcement of the materials. Due to the incompatibility of hydrophilic layered silicates and hydrophobic polymer matrix, the individual nanolayers are not easily separated and dispersed in many polymers. For this purpose, silicate layers are usually modified with an intercalating agent to obtain organically modified clay prior to use in nanocomposite formation [12, 13]. The performance of polymer nanocomposite using organically modified clays varies depending on the level of dispersion, the alkyl ammonium ions and the silicates present in the clay, and the polymer type [14–18].

Also aromatic polyimides are used extensively as a class of high performance materials due to their remarkable thermal and oxidative stabilities and excellent electrical and mechanical properties for long time period [19]. The strong interaction between polyimide chains and their rigid structure make them intractable. Poor thermoplastic fluidity and solubility are the major problems for wide application of polyimides. Thus, to overcome these processing problems various approaches have been carried out by incorporating flexible units such as –NHCO–, –O–, and $–SO_2–$ [20–22]. In this article two PAI-nanocomposite films with 10 and 20 mass % silicate particles containing chiral(4-N-trimellitylimido)diphenyl ether moiety in the main chain was prepared by using a convenient solution intercalation technique. In this article two PAI-nanocomposite films with 10 and 20 mass % silicate particles containing chiral(4-N-trimellitylimido)diphenyl ether moiety in the main chain was prepared by using a convenient solution intercalation technique.

Corresponding author: Khalil Faghihi, Polymer Research Laboratory, Department of Chemistry, Faculty of Science, Islamic Azad University, Arak Branch, Arak, Iran; E-mail: k-faghihi@araku.ac.ir.

Received: October 22, 2010. Accepted: November 12, 2010.

2 Experimentals

2.1 Materials

Trimellitic dianhydride, 4,4'-diamino diphenyl ether, acetic acid, triphenyl phosphite (TPP), $CaCl_2$, pyridine and N-

methyl-2-pyrrolidone (NMP) were purchased from Merck Chemical Company and used without previous purification.

2.2 Measurements

^{1}H-NMR spectrum was recorded on a Bruker 300 MHz instrument (Germany). Fourier transform infrared (FTIR) spectra were recorded Vibration transition frequencies were reported in wave number ($cm^{-1} = 10^{-2}\ m^{-1}$) on Galaxy Series FTIR 5000 spectrophotometer (England). UV-visible spectra were recorded at 298 K (25 °C) in the 250–700 nm spectral regions with a Perkin Elmer Lambda 15 spectrophotometer in NMP solution using cell lengths of 1 cm. Thermal Gravimetric Analysis (TGA and DTG) data were taken on a Mettler TA4000 System under N_2 atmosphere at a rate of 10 K/min. The morphology of nanocomposite film was investigated on Canbridge S260 scanning electron microscope (SEM).

2.3 Monomer and Polymer Syntheses

For monomer synthesis, Bis (4-N-trimellitylimido)diphenyl ether 3 was prepared according to a typical procedure is shown in Figure 1 in [23].

For polymer synthesis, Into a 100 mL round bottomed flask were placed a mixture of Bis (4-N-trimellitylimido)diphenyl ether 3 (0.002 mol), 4,4'-diamino diphenyl ether 2 (0.002 mol), 0.60 g of calcium chloride, 1.0 mL of triphenyl phosphite, 1.0 mL of pyridine and 4.0 mL NMP. The mixture was heated for 12 h at 393 K (120 °C) until a viscous solution was formed. Then it was cooled to room temperature and 30 mL of methanol was added to reaction mixture. The precipitate was formed, filtered off and washed with hot methanol. The resulting polymers 4 were dried under vacuum. The inherent viscosity of this soluble PAI 4 was 0.59 m^3/kg.

2.4 PAI-Nanocomposite Synthesis 4a and 4b

PAI-nanocomposites 4a and 4b were produced by solution intercalation method, in two different amounts of organoclay particles (10 and 20 mass %) were mixed with appropriate amounts of PAI solution in N-methyl-2-pyrrolidone (NMP) to yield particular nanocomposite concentrations. To control the dispersibility of organoclay in poly(amide-imide) matrix, constant stirring was applied at 298 K (25 °C) for 24 h. Nanocomposite films were cast by pouring the solutions for each concentration into petri dishes placed on a leveled surface followed by the evaporation of solvent at 343 K (70 °C) for 12 h. Films were dried at 353 K (80 °C) under vacuum to a constant weight. Scheme 1 show the flowsheet diagram and synthetic scheme for PAI-nanocomposites film 4a and 4b.

2.5 The Water Absorption Analysis

The water absorption of PAI-nanocomposite films was carried out using a procedure under ASTM D570-81 [24]. The films were dried in a vacuum oven at 378 K (80 °C) to a constant weight and then weighed to get the initial weight (W_0). The dried films were immersed in deionized water at 298 K (25 °C). After 24 h, the films were removed from water and then they were quickly placed between sheets of filter paper to remove the excess water and films were weighed immediately. The films were again soaked in water. After another 24 h soaking period, the films were taken out, dried and weighed for any weight gain. This process was repeated again and again till the films almost attained the constant weight. The total soaking time was 168 h and the samples were weighed at regular 24 h time intervals to get the final weight (W_f). The percent increase in weight of the samples was calculated by using the formula $(W_f - W_0)/W_0$.

3 Results and Discussion

3.1 Monomer Synthesis

Bis (4-N-trimellitylimido)diphenyl ether 3 was synthesized by the condensation reaction of trimellitic anhydride 1 with 4,4'-diamino diphenyl ether 2 in an acetic acid solution (Figure 1).

The chemical structure of diacid 3 was confirmed by FT-IR and ^{1}H-NMR spectroscopy. In the FT-IR spectrum of diacid 3 peaks appearing at 2500–3400 cm^{-1} (acid O-H stretching), 1774 cm^{-1}($cm^{-1} = 10^2\ m^{-1}$) (C=O asymmetric imide stretching), 1620 and 1723 cm^{-1} (C=O acid and symmetric imide stretching), 1386 and 724 cm^{-1} (imide characteristic ring vibration) confirmed the presence of imide ring and carboxylic groups in this compound. The ^{1}H-NMR spectrum of diacid 3 shows H(a) protons relevant to O-H carboxylic groups and peaks between 7.24 and 7.50 related to aromatic protons diphenyl ether. Peaks in region 8.05–8.38 related to aromatic protons trimellitic anhydride.

3.2 Polymer Synthesis

Poly(amide-imide)s 4 was synthesized by the direct solution polycondensation reaction of an equimolar mixture of diacid 3, an equimolar mixture of diamine 2 by using triphenyl phosphite (TPP) and pyridine as condensing agents (Figure 2). PAI 4 was obtained in good yield (94 %) and inherent viscositiy (0.59 m^3/kg). The structure of resulting polymer 4 was confirmed as PAI by using FT-IR spectroscopy and elemental analyses. The resulting polymer have absorption band between 1773 and 1659 cm^{-1} due to imide and amide carbonyl groups. Absorption bands around 1376 cm^{-1} and 721 cm^{-1} demonstrated the presence of the

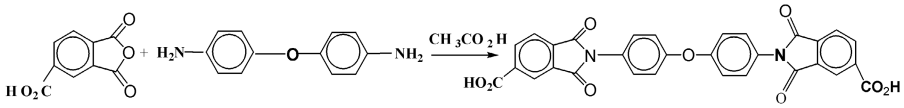

Figure 1. Synthetic route of Bis (4-N-trimellitylimido)diphenyl ether 3.

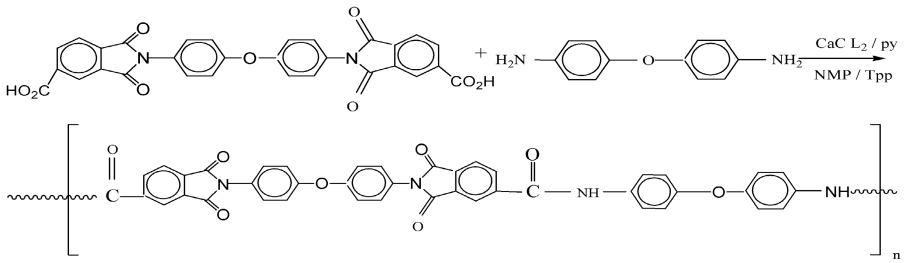

Figure 2. Synthetic route of PAI 4.

imide heterocyclic absorption in these polymers. Also absorption band of amide group appeared at 3485 cm^{-1} (N-H stretching). The elemental analysis value of the resulting polymer was in good agreement with the calculated values for the proposed structure.

3.3 PAI-Nanocomposite Films

PAI-nanocomposite films were transparent and yellowish brown in color. The incorporation of organoclay changed the color of films to dark yellowish brown. Moreover, a decrease in the transparency was observed at higher clay contents. Figure 3 shows the flow sheet diagram and synthetic scheme for PAI-nanocomposites film 4a and 4b.

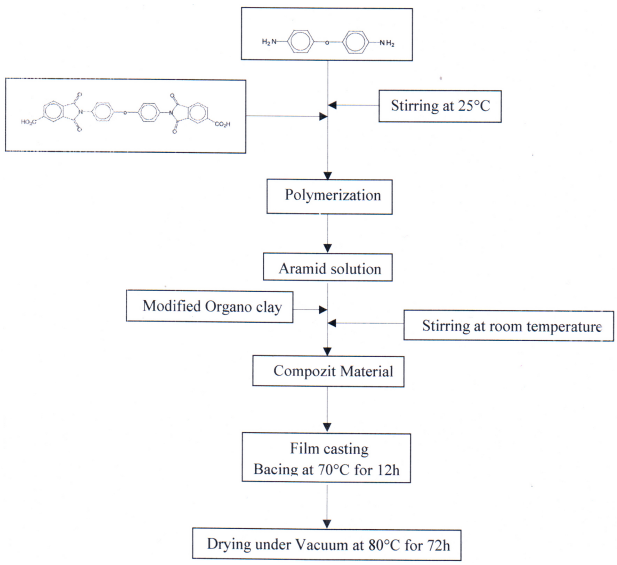

Figure 3. Flow sheet diagram for the synthesis of PAI-nanocomposites film 4a and 4b.

3.4 Characterization

3.4.1 FT-IR Spectroscopy Analyses

FT-IR spectroscopy spectra of PAI-nanocomposite films 4a and 4b showed the characteristic absorption bands of the Si-O and Mg-O moieties at 1080, 514 and 459 cm^{-1} respectively. The incorporation of organic groups in PAI-nanocomposite films was confirmed by the presence of peaks at 1774, 1717, 719 cm^{-1} (imide rings) and 1650 (amide carbonyl group) from the results of Figure 4.

3.4.2 X-Ray Diffraction Analysis

Figure 5 shows the XRD patterns of PAI-nanocomposite films 4a and 4b containing 10 and 20- mass % of silicate particles. The result reveals an increased d-spacing from 1.00 nm (8.78 °) of Na-MMT to 1.49 nm (5.70 °) of PAI-nanocomposite film (10 mass %) and (4.25 °) of PAI-nanocomposite film (20 mass %). These results indicated significant expansion of the silicate layer after insertion PAI chains. The shift in the diffraction peaks PAI-nanocomposite films confirms that intercalation has been taken place. This is direct evidence that PAI-nanocomposites have been formed as the nature of intercalating agent also affects the organoclay dispersion in the polymer matrix. Usually there are two types of nanocomposites depending upon the dispersion of clay particles. The first type is an intercalated polymer clay nanocomposite, which consists of well ordered multi layers of polymer chain and silicate layers a few nanometers thick. The second type is an exfoliated polymer-clay nanocomposite, in which is there is a loss of ordered structures due to the extensive penetration of polymer chain into the layer silicate. Such part would not produce distinct peaks in the XRD pattern [25]. In our PAI- nanocomposite films there are coherent XRD signal at 5.70 ° and 4.25 ° related to 10 and 20 mass % nanocomposite films respectively.

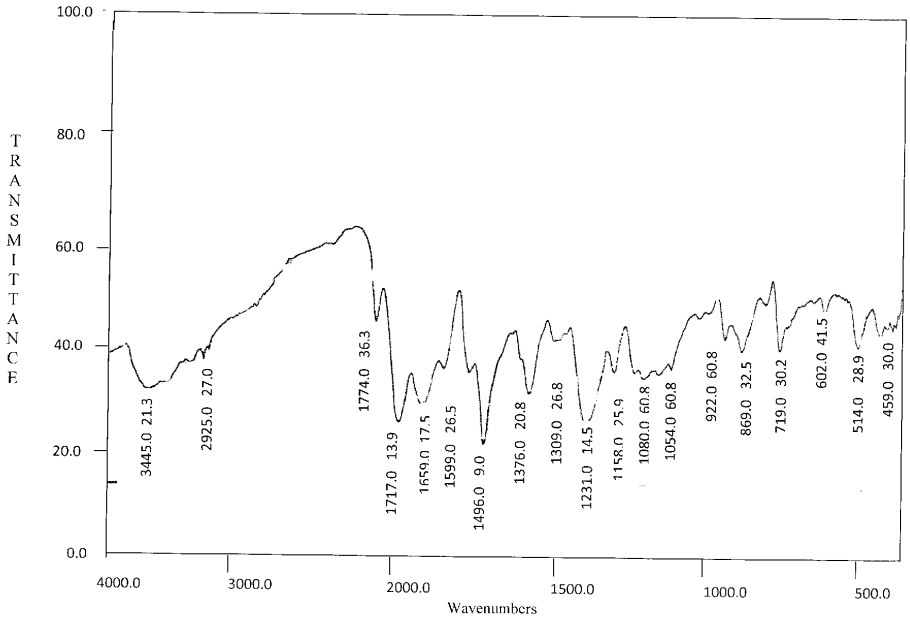

Figure 4. FT-IR spectrum of PAI-nanocomposite films 4a.

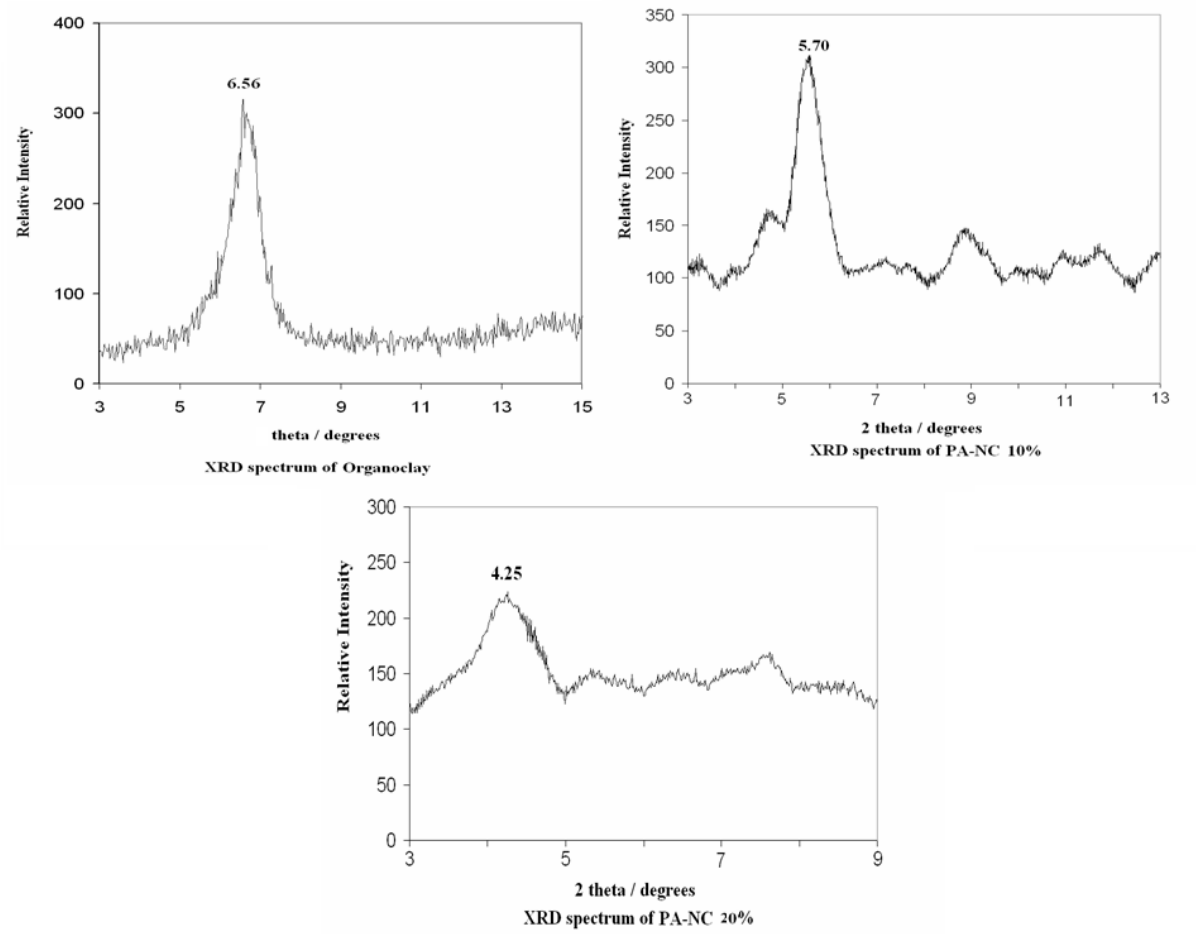

Figure 5. X-ray diffraction patterns of Organoclay (a), PAI-nanocomposite films 4a (b) and 4b (c).

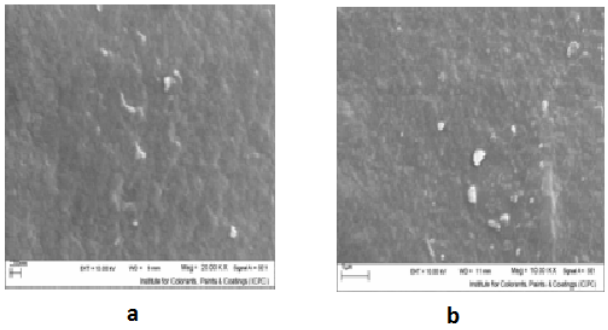

Figure 6. Scanning electron micrographs of PAI-nanocomposite films 4a (a) and 4b (b).

3.4.3 Scanning Electron Microscopy

The surface morphology of the PAI-nanocomposite films prepared by solution intercalation technique is compared by SEM analyses. Figure 6 shows the morphological images of 10 and 20 mass % nanocomposite films respectively. The SEM images show that PAI matrix has a smooth morphology, where as the PAI matrix has an amorph morphology. Also SEM micrographs of PAI-nanocomposite containing 10 and 20 mass % clay platelets were uniformly distributed without agglomeration.

3.4.4 Optical Clarity of PAI-Nanocomposite Films

Optical clarity of PAI-nanocomposite films containing 10 and 20 mass % clay platelets and neat PAI was compared by Uv-vis spectroscopy in the region of 200–700 nm. Figure 7 show the UV-vis transmission spectra of pure PAI and PAI-nanocomposite films containing 10 and 20 mass % clay platelets. These spectra show that the UV-visible region (250–700 nm) is affected by the presence of the clay particles and exhibiting low transparency reflected to the primarily intercalated composites. Results shows that the optical clarity of PAI-nanocomposite films system is significantly lower the neat PAI system.

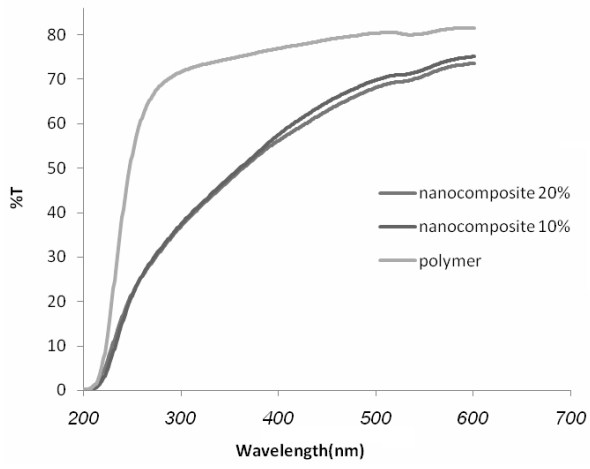

Figure 7. Uv-vis spectra of PAI4, PAI-nanocomposite films 4a and 4b.

3.4.5 Thermogravimetric Analysis

The thermal properties of PAI-nanocomposite films containing 10 and 20 mass % clay platelets and neat PAI were investigated by using TGA and DTG in nitrogen atmosphere at a rate of heating of 10 °K/min, and thermal data are summarized in Table 1. These samples exhibited good resistance to thermal decomposition, up to 200–250 °C (= 473–523 K) in nitrogen, and began to decompose gradually above this temperature. T_5 for these polymers ranged from 200–250 °C (= 473–523 K) and T_{10} for them ranged from 250–425 °C (= 523–698 K), and residual weights at 600 °C (= 873 K) ranged from 64.46 and 74.52 % in nitrogen respectively. Incorporation of organoclay into the PAI matrix also enhanced the thermal stability of the nanocomposites. Figure 8 shows the TGA thermograms of PAI-nanocomposites under nitrogen atmosphere. Thus, we can speculate that interacting PAIs chains between the clay layers serve to improve the thermal stability of nanocomposites. The addition of organoclay in polymeric matrix can significantly improve the thermal stability of PAI.

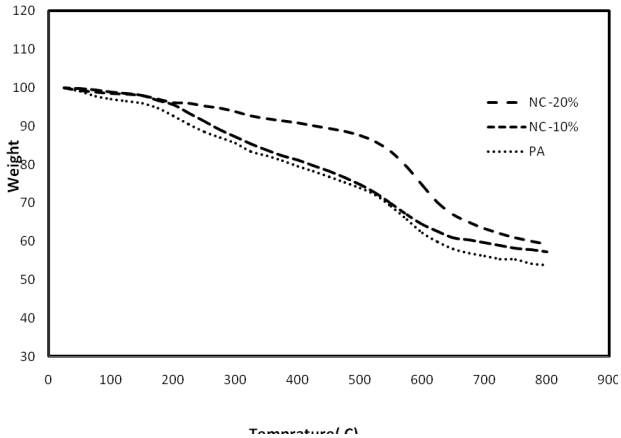

Figure 8. TGA thermograms of neat PAI 4 and PAI-nanocomposite films 4a and 4b.

3.4.6 Water Absorption Measurements

The PAI under investigation contains polar and cyclic imide rings and also polar amide groups in the backbone that have the tendency to uptake water through hydrogen bonding. Thus water absorption measurements become necessary for neat PAI 4 and PAI-nanocomposite films 4a and 4b and data are shown in Table 1. In the water permeability studies, we found that the incorporation of clay platelets into PAI matrix results in a decrease of water uptake relative to pure PAI by forming the tortuous path of water permeant. Wa-

Polyimide	T_5(°K) [a]	T_{10}(°K) [b]	Char Yield [c]	Water uptake (%)
4	448	498	62.22	5.7
4a	573	523	64.46	1.6
4b	523	698	74.52	0.5

[a,b] Temperature at which 5 % and 10 % weight loss was recorded by TGA at heating rate of 10 °C/min in N_2 respectively;

[c] Percentage weight of material left undecomposed after TGA analysis 600 °C (= 873 K).

Table 1. Thermal behaviors and Water uptake of neat PAI 4 and PAI-nanocomposite films 4a and 4b.

ter permeability depends on length, orientation and degree of delamination of layered silicate [26]. It should be noted that a further increase in clay concentration resulted in an enhanced barrier property of nanocomposites which may be attributed to the plate-like clays that effectively increase the length of the diffusion pathways, as well as decrease the water permeability.

4 Conclusions

The PAI-nanocomposites were successfully prepared using solution intercalation method. The structure and the uniform dispersion of organoclay throughout the PAI matrix were confirmed by FTIR, XRD and SEM analyses. The optical clarity and water absorption property of PAI-nanocomposites were deccreased significantly with increasing the organoclay contents in PAI matrix. On the contrary the thermal stability of PAI-nanocomposites were inccreased significantly with increasing the organoclay contents in PAI matrix. The enhancements in the thermal stability of the nanocomposites films 4a and 4b caused by introducing organoclay may be due to the strong interactions between polymeric matrix and organoclay generating well intercalation and dispersion of clay platelets in the PAI matrix.

References

[1] S. Zulfiqar and M.I. Sarwar, *Scr. Mater.*, **59** (2008), 436–439.

[2] Y. Yano, A. Usuki, T. Kurauchi and O. Kamigato, *J. Polym. Sci. Part A: Polym. Chem.*, **31** (1993), 2493–2498.

[3] S. Zulfiqar, Z. Ahmad, M. Ishaq, S. Saeed and M. I. Sarwar, *J. Mater. Sci.*, **42** (2007), 93–100.

[4] E. P. Giannelis, *Adv. Mater.*, **8** (1996), 29–35.

[5] M. Sikka, L. N. Cerini, S. S. Ghosh and K. I. Winey, *J. Polym. Sci. Part B: Polym. Phys.*, **34** (1996), 1443–1449.

[6] C. Zilg, R. Mulhaupt and J. Finter, *Macromol. Chem. Phys.*, **200** (1999), 661–670.

[7] P. B. Messersmith and E. P. Giannelis, *Chem. Mater.*, **6** (1994), 1719–1725.

[8] R. Xu, E. Manias, A. J. Snyder and J. Runt, *Macromolecules,* **34** (2001), 337–339.

[9] S. D. Burnside and E. P. Giannelis, *Chem. Mater.,* **7** (1995), 1597–1600.

[10] A. Kausar, S. Zulfiqar, S. Shabbir, M. Ishaq and M. I. Sarwar, *Polym. Bull.*, **59** (2007), 457–468.

[11] N. Bibi, M. I. Sarwar, M. Ishaq and Z. Ahmad, *Polym. Polym. Compos.*, **15** (2007), 313–319.

[12] G. M. Chen, Y. M. Ma and Z. N. Qi, *J. Appl. Polym. Sci.*, **77** (2000), 2201–2205.

[13] Y. Yano, A. Usuki, T. Kurauchi and O. Kamigato, *J. Polym. Sci. Part A: Polym. Chem.*, **31** (1993), 2493–2498.

[14] J. M. Yeh, C. L. Chen, T. H. Kuo, W. F. Su, H. Y. Huang, D. J. Liaw, H. Y. Lu, C. F. Liu and Y. H. Yu, *J. Appl. Polym. Sci.*, **92** (2004), 1072–1079.

[15] A. Gu, S. W. Kuo and F. C. Chang, *J. Appl. Polym. Sci.*, **79** (2001), 1902–1910.

[16] C. Nah, S. H. Han, J. H. Lee, M. H. Lee, S. D. Lim and J. M. Rhee, *Compos. Part B,* **35** (2004), 125–131.

[17] M. C. Lai, G. W. Jang, K. C. Chang, S. C. Hsu, M. F. Hsieh and J. M. Yeh, *J. Appl. Polym. Sci.*, **109** (2008), 1730–1737.

[18] T. Agag, T. Koga and T. Takeichi, *Polymer,* **42** (2001), 3399–3408.

[19] C. H. Ju, J. C. Kim and J. H. Chang, *J. Appl. Polym. Sci.*, **106** (2007), 4192–4201.

[20] A. Kausar, S. Zulfiqar, S. Shabbir, M. Ishaq and M. I. Sarwar, *Polym. Bull.*, **59** (2007), 457–468.

[21] Kh. Faghihi, M. Shabanian and M. Hajibeygi, *Macromol. Res.*, **17** (2009), 912–918.

[22] Kh. Faghihi, M. Hajibeygi and M. Shabanian, *Macromol. Res.*, **17** (2009), 739–745.

[23] Kh. Faghihi and M. Hajibeygi, *J. Appl. Polym. Sci.*, **92** (2004), 3447–3453.

[24] S. Zulfiqar and M. I. Sarwar, *J. Incl. Phenom. Macrocycl. Chem.*, **62** (2008), 353–361.

[25] P. S. G. Krishnan, A.E. Wisanto, S. Osiyemi and C. Ling, *Polym. Inter.*, **56** (2007), 787–795.

[26] R. K. Bharadwaj, *Macromolecules*, **34** (2001), 9189–9192.